Electronic Supplementary Materials 3 (ESM3) – Additional results and methodological details of the musculoskeletal model

This document is an electronic supplementary material (ESM3) for the article entitled "Electromyography-informed musculoskeletal modelling provides new insight into hand tendon forces during tennis forehand"

Article information

Electromyography-informed musculoskeletal modelling provides new insight into hand tendon forces during tennis forehand

Goislard de Monsabert B[a]*, Herbaut A[b], Cartier T[a], Vigouroux L[a].

[a]*Aix-Marseille University, CNRS, ISM, Marseille, France;* [b]*Movement Sciences Department, Decathlon SportsLab Research and Development, Villeneuve d'Ascq, France*

*Corresponding author: Benjamin Goislard de Monsabert, Ph.D. benjamin.goislard-de-monsabert@univ-amu.fr.

Table of contents

Musculoskeletal model additional results

Wrist net moment components

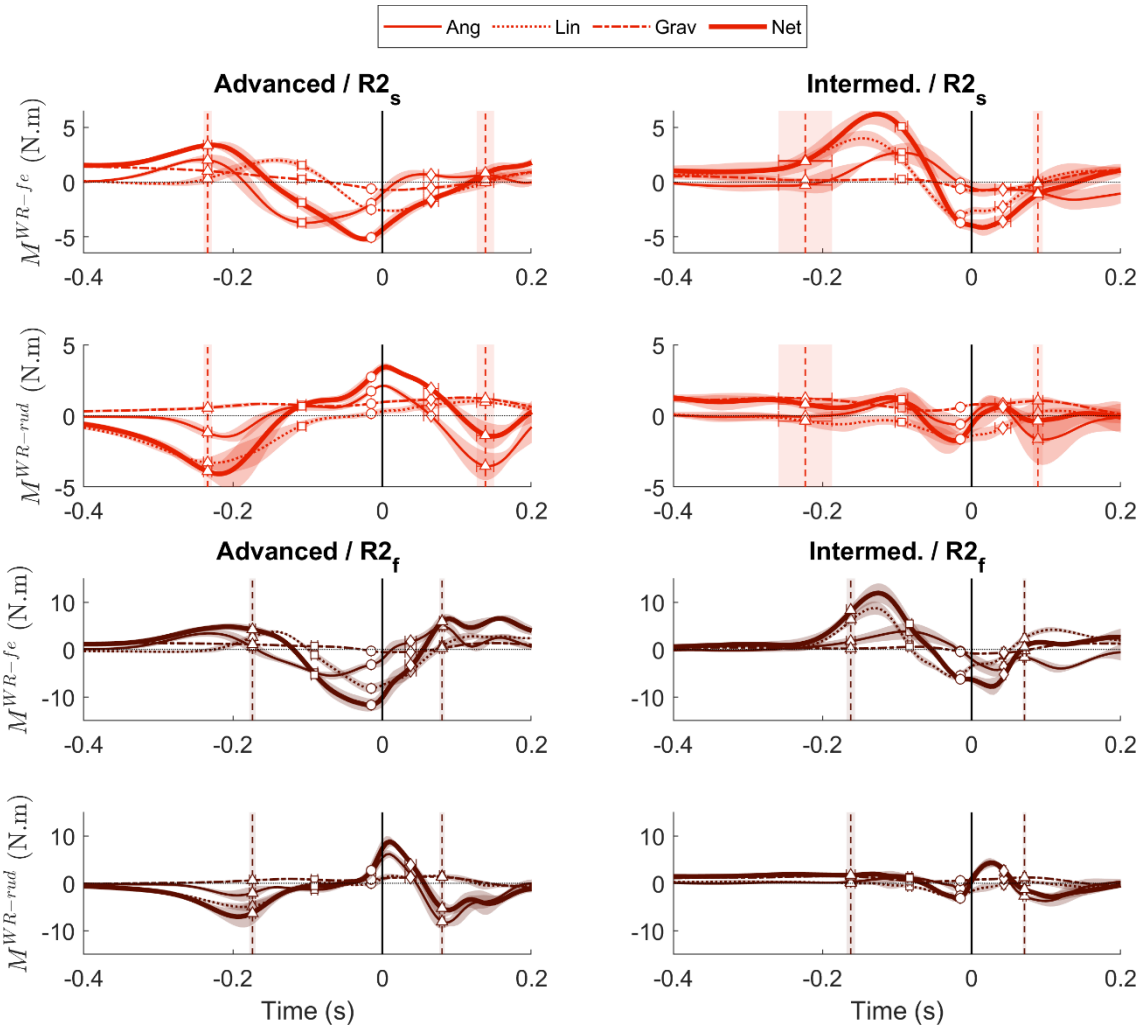

Figure s3-1. Mean time-patterns (N=5 trials) of wrist net moment components during the forehand drive of both players (Advanced and Intermediate) for the two shot speeds (Slow, s; Fast, s) performed with the racket R2. Shaded areas represent ± one standard deviations around the mean. Lighter nuances represent the Slow (s) speed shots and darker nuances the Fast (f) ones. The vertical solid black bar represents the impact frame, the dashed vertical bars represent the beginning and end of forward acceleration phase, and the different points correspond to the frames on which musculoskeletal model was ran (see corpus of the article). Ang: angular acceleration moment component; Lin: Linear acceleration moment component; Grav: gravitation moment component; Net: sum of three components

Muscle forces and lengths estimated via Force-Length-Activation models

The following two graphs present the data estimated via the muscle-specific Force-Length-Activation models from joint angle and muscle activation used to provide EMG-informed guidance to the inverse-dynamics musculoskeletal model (see corpus). The model details can be found at the end of this document.

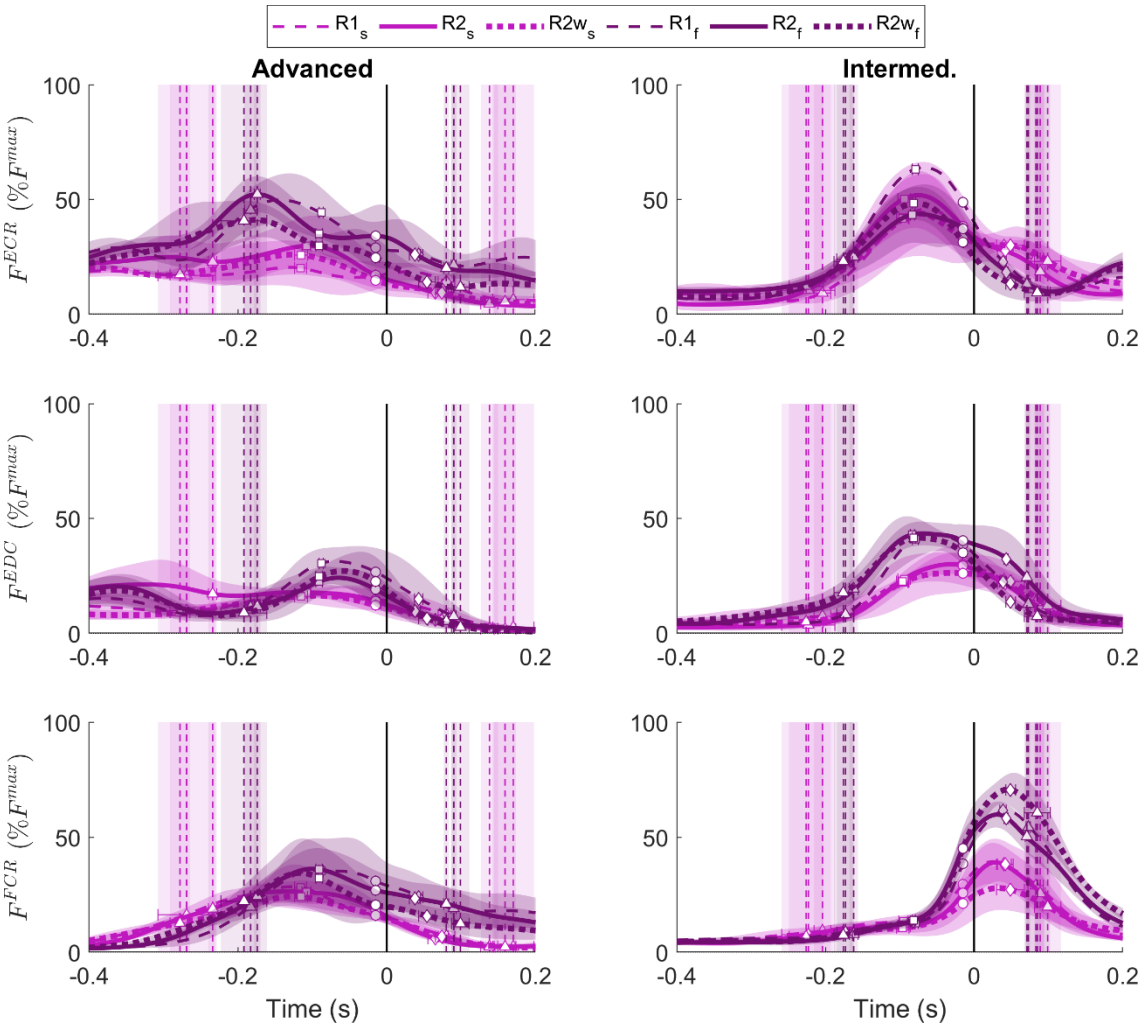

Figure s3-2. Mean time-patterns (N=5 trials) of muscle forces estimated using the muscle-specific Force-Length-Activation models during the forehand drive of both players (Advanced and Intermediate) for the two shot speeds (Slow, s; Fast, s) performed with the three rackets (R1, R2, R2w). Shaded areas represent ± one standard deviations around the mean. Lighter nuances represent the Slow (s) speed shots and darker nuances the Fast (f) ones. The vertical solid black bar represents the impact frame, the dashed vertical bars represent the beginning and end of forward acceleration phase, and the different points correspond to the frames on which musculoskeletal model was ran (see corpus of the article). ECR: extensor carpi radialis, EDC: extensor digitorum communis, FCR: flexor carpi radialis.

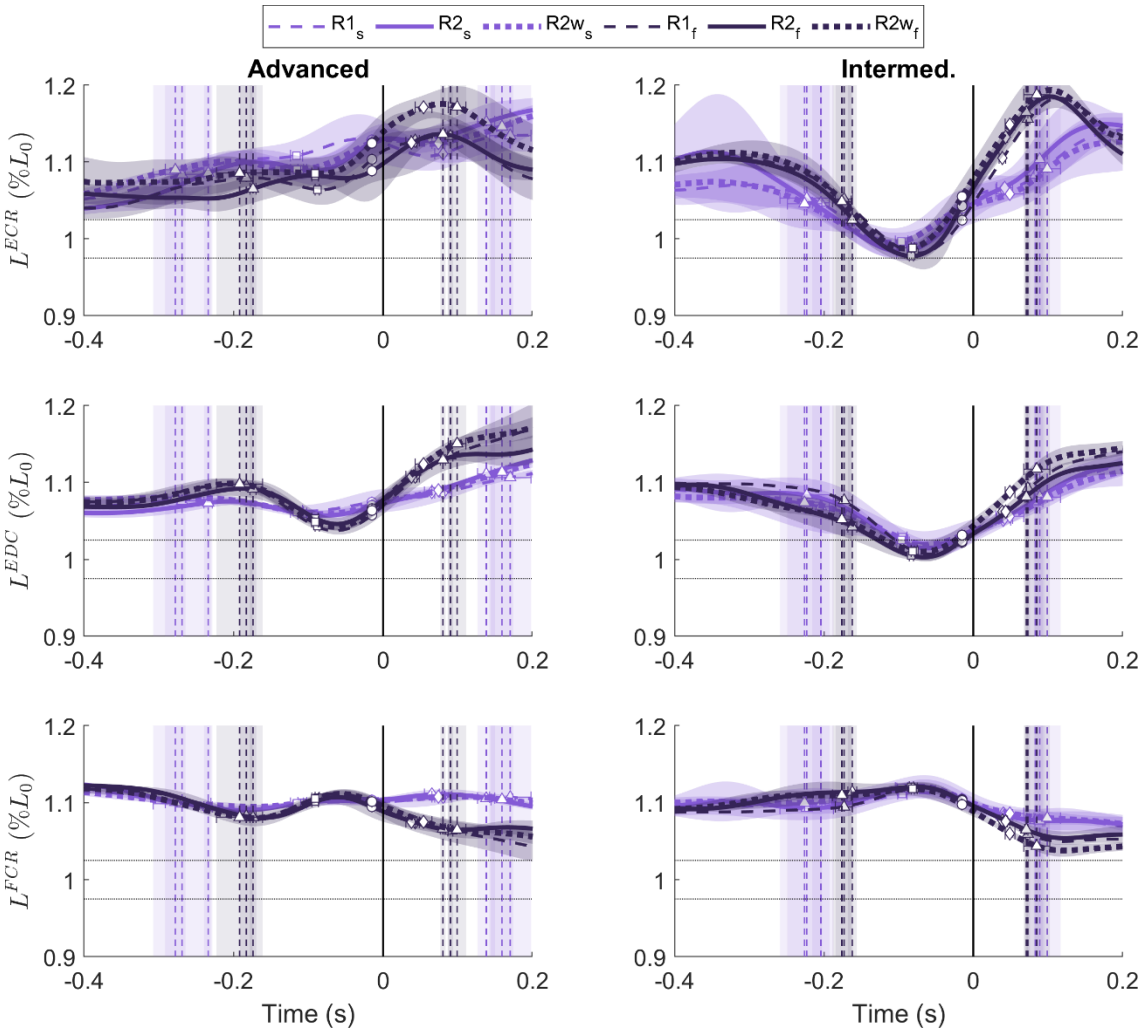

Figure s3-3. Mean time-patterns (N=5 trials) of muscle lengths estimated using the muscle-specific Force-Length-Activation models during the forehand drive of both players (Advanced and Intermediate) for the two shot speeds (Slow, s; Fast, s) performed with the three rackets (R1, R2, R2w). Shaded areas represent ± one standard deviations around the mean. Lighter nuances represent the Slow (s) speed shots and darker nuances the Fast (f) ones. The vertical solid black bar represents the impact frame, the dashed vertical bars represent the beginning and end of forward acceleration phase, and the different points correspond to the frames on which musculoskeletal model was ran (see corpus of the article). ECR: extensor carpi radialis, EDC: extensor digitorum communis.

Muscle forces estimated by the EMG-informed musculoskeletal model

The two figures on the next pages present all the 42 individual muscle forces estimated by the EMG-informed musculoskeletal model. The six rows of figures represent the muscle forces at the thumb, at the index, middle, ring and little fingers and at the wrist, respectively. The muscle abbreviations are detailed in the table below.

Table s3-1 – List of muscles included in the EMG-informed musculoskeletal model, their abbreviation, and their corresponding muscle group

	Abb.	Definition	Type	Group
Thumb				
	FPL	Flexor pollicis longus	Extrinsic	-
	FPB	Flexor pollicis brevis	Intrinsic	-
	OPP	Opponens pollicis	Intrinsic	-
	APB	Abductor pollicis brevis	Intrinsic	-
	ADPt	Aductor pollicis transverse head	Intrinsic	-
	ADPo	Aductor pollicis oblique head	Intrinsic	-
	APL	Abductor pollicis longus	Extrinsic	-
	EPL	Extensor pollicis longus	Extrinsic	-
	EPB	Extensor pollicis brevis	Extrinsic	-
Index				
	FDP2	Flexor digitorum profundus index finger compartment	Extrinsic	F-flex
	FDS2	Flexor digitorum superficialis index finger compartment	Extrinsic	F-flex
	LU2	Lumbrical of index finger (1st lumbrical)	Intrinsic	-
	RI2	Radial interosseus of index finger (1st dorsal interosseus)	Intrinsic	-
	UI2	Ulnar interosseous of index finger (1st palmar interosseus)	Intrinsic	-
	EDC2	Extensor digitorum communis index finger compartment	Extrinsic	F-ext
	EDI	Extensor indicis	Extrinsic	-
Middle				
	FDP3	Flexor digitorum profundus middle finger compartment	Extrinsic	F-flex
	FDS3	Flexor digitorum superficialis middle finger compartment	Extrinsic	F-flex
	LU3	Lumbrical of middle finger (2nd lumbrical)	Intrinsic	-
	RI3	Radial interosseus of middle finger (2nd dorsal interosseus)	Intrinsic	-
	UI3	Ulnar interosseous of middle finger (3rd dorsal interosseus)	Intrinsic	-
	EDC3	Extensor digitorum communis middle finger compartment	Extrinsic	F-ext
Ring				
	FDP4	Flexor digitorum profundus ring finger compartment	Extrinsic	F-flex
	FDS4	Flexor digitorum superficialis ring finger compartment	Extrinsic	F-flex
	LU4	Lumbrical of ring finger (3rd lumbrical)	Intrinsic	-
	RI4	Radial interosseus of ring finger (2nd palmar interosseus)	Intrinsic	-
	UI4	Ulnar interosseous of ring finger (4th dorsal interosseus)	Intrinsic	-
	EDC4	Extensor digitorum communis ring finger compartment	Extrinsic	F-ext
Little				
	FDP5	Flexor digitorum profundus little finger compartment	Extrinsic	F-flex
	FDS5	Flexor digitorum superficialis little finger compartment	Extrinsic	F-flex
	FDQ	Flexor digit quinti	Intrinsic	-
	LU5	Lumbrical of little finger (4th lumbrical)	Intrinsic	-
	RI5	Radial interosseus of little finger (3rd palmar interosseus)	Intrinsic	-
	UI5	Ulnar interosseous of little finger (abductor digiti quinti)	Intrinsic	-
	EDC5	Extensor digitorum communis little finger compartment	Extrinsic	F-ext
	EDQ	Extensor digit quinti	Extrinsic	-
Wrist				
	FCR	Flexor carpi radialis	Wrist mover	W-flex
	FCU	Flexor carpi ulnaris	Wrist mover	W-flex
	PL	Palmaris longus	Wrist mover	W-flex
	ECRB	Extensor carpi radialis brevis	Wrist mover	W-ext
	ERCL	Extensor carpi radialis longus	Wrist mover	W-ext
	ECU	Extensor carpi ulnaris	Wrist mover	W-ext

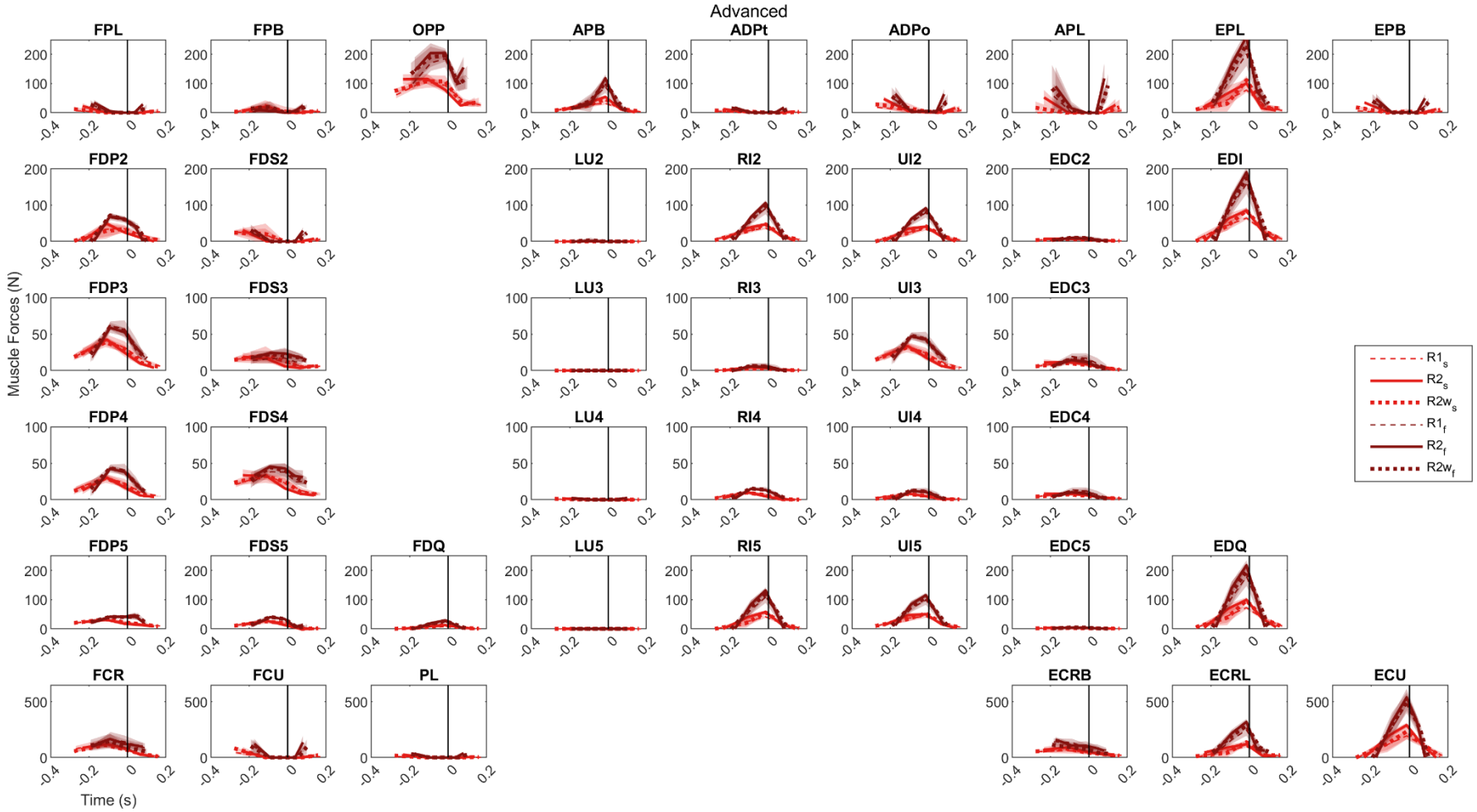

Figure s3-4. Mean time-patterns (N=5 trials) of muscle forces estimated by the EMG-informed musculoskeletal during the forehand drive for the Advanced player the for the two shot speeds (Slow, s; Fast, s) performed with the three rackets (R1, R2, R2w). Shaded areas represent ± one standard deviations around the mean. Lighter nuances represent the Slow (s) speed shots and darker nuances the Fast (f) ones. The vertical solid black bar represents the impact frame, the dashed vertical bars represent the beginning and end of forward acceleration phase, and the different points correspond to the frames on which musculoskeletal model was ran (see corpus of the article). Muscle abbreviations are defined in the table above

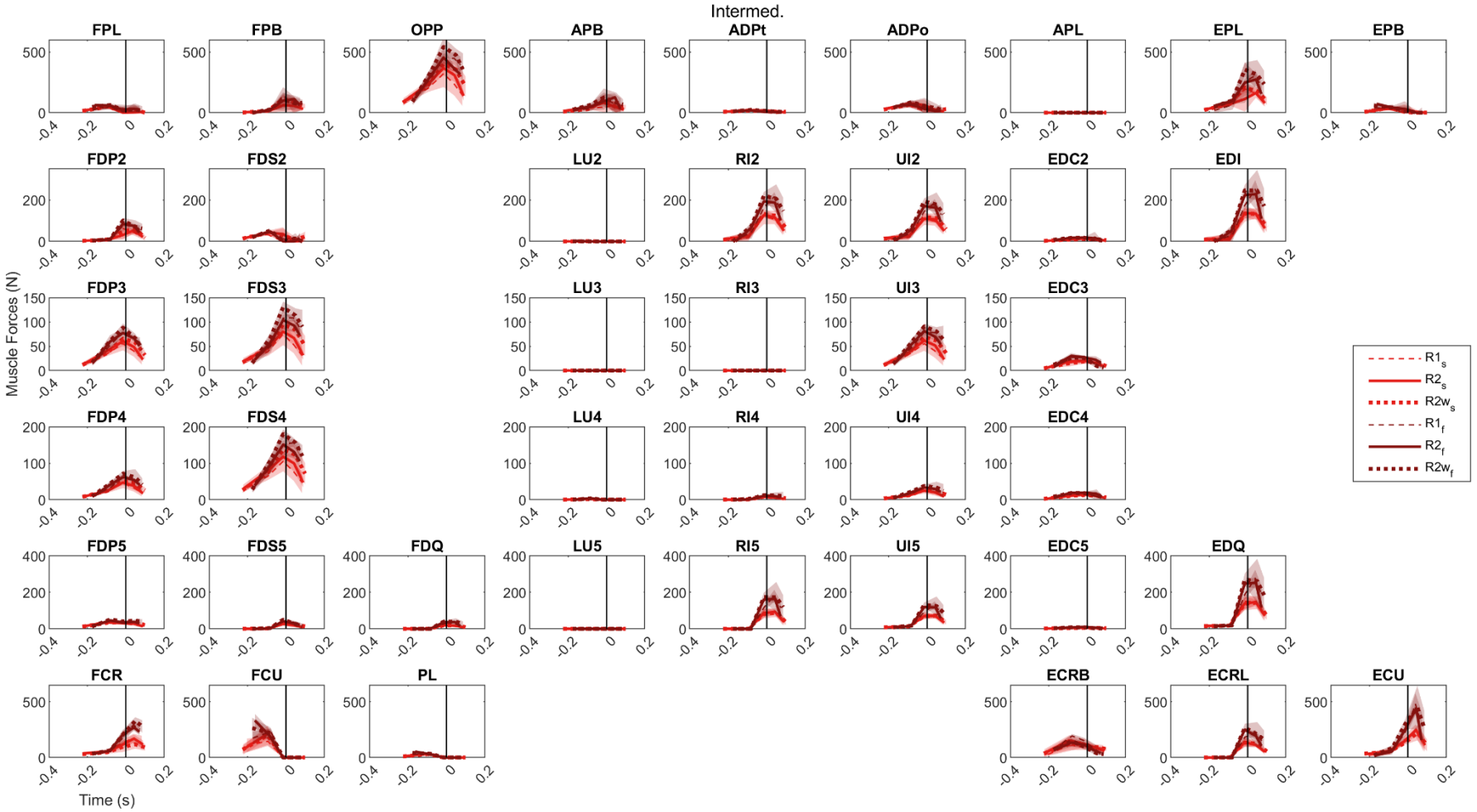

Figure s3-5. Mean time-patterns (N=5 trials) of muscle forces estimated by the EMG-informed musculoskeletal during the forehand drive for the Interemdiate player the for the two shot speeds (Slow, s; Fast, s) performed with the three rackets (R1, R2, R2w). Shaded areas represent ± one standard deviations around the mean. Lighter nuances represent the Slow (s) speed shots and darker nuances the Fast (f) ones. The vertical solid black bar represents the impact frame, the dashed vertical bars represent the beginning and end of forward acceleration phase, and the different points correspond to the frames on which musculoskeletal model was ran (see corpus of the article). Muscle abbreviations are defined in the table above

Sensitivity analysis

A sensitivity analysis was run to quantify how the estimated muscle forces are affected by a modification of ±15% of each of the experimental data inputted in the EMG-informed musculoskeletal model. The data presented below correspond to the variations of muscle forces at the Pre-Impact frame of a single trial of the Advanced player performing a Fast shot with the R2 racket. The figure below presents the results of modifying eight input data, listed below.

- F^{grip}: grip force estimated using FDS activation
- θ^{WR-fe}: wrist flexion-extension joint angle
- θ^{WR-rud}: wrist radial ulnar joint angle
- M^{WR-fe}: wrist flexion-extension net moment
- M^{WR-rud}: wrist radial-ulnar net moment
- F^{FCR} : FCR muscle force estimated using the Force-Length-Activation model
- F^{ECR} : FCR muscle force estimated using the Force-Length-Activation model
- F^{EDC} : EDC muscle force estimated using the Force-Length-Activation model

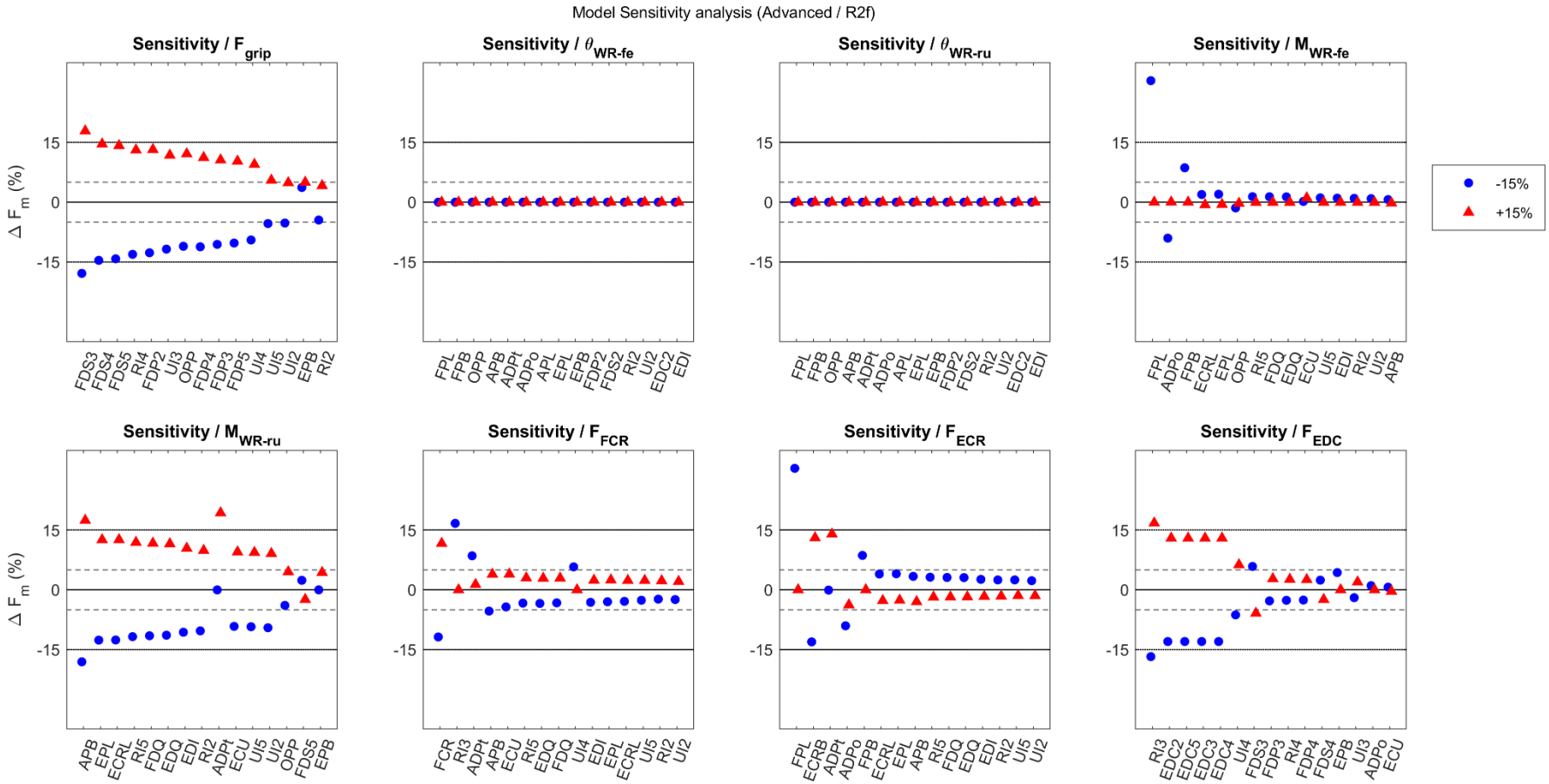

Figure s3-6. Normalized muscle force variations induced by ±15% modification of each of the eight experimental input data (see list above). The analysis was run for a single trial of the Advanced player performing a Fast shot with the R2 racket and only the variations at Pre-Impact frame are shown. Variations are expressed as difference between perturbed (±15% input modification) and nominal trial (no modification), expressed as percentage of the highest force estimated in the nominal trial for that muscle. For each modified input variable, only the 15 muscles with the highest variations are shown.

EMG-informed musculoskeletal model methodological details

Force-length-activation model

The EMG-informed musculoskeletal model was guided by estimations of muscle forces from electromyography and joint angles, i.e., a forward dynamics model. This model was based on Force-Length-Activation relationships and was used to estimate the force (F^m) of *extensor digitorum communis* (EDC), *flexor carpi radialis* (FCR) and *extensor carpi radialis* (ECR). The model was divided in three steps (Figure s3-7): muscle-tendon unit kinematics, muscle belly excursion, and force-length-activation relationships. The equations and data corresponding to muscle belly excursion and force-length-activation were taken from previous studies (Goislard de Monsabert et al., 2020; Hauraix et al., 2018) that combined motion capture, ergometer, ultrasound imaging and electromyography data during maximal isometric contractions.

Step 1 - Muscle-tendon unit kinematics

The current muscle-tendon unit (MTU) length (L^{mtu}) was determined from the measured reference MTU length (L_r^{mtu}) and joint angles (θ^j) using geometrical models representing the path of the tendon around each joint as a function of was current angular position. The current MTU length was calculated by adding to L_r^{mtu} the total MTU excursion corresponding to the sum of excursion at each individual joint (ΔL_j^{mtu}).

$$L^{mtu} = L_r^{mtu} + \sum_j \Delta L_j^{mtu} \qquad \text{Equation 1}$$

With j corresponding to one of the four joints, i.e., wrist (WR) and index finger distal (DIPi) or proximal (PIPi) interphalangeal or metacarpophalangeal (MCPi) joint. The excursion was null when tendon was not crossing the joint such that $\Delta L_{DIPi}^{MTU} = \Delta L_{PIPi}^{MTU} = \Delta L_{MCPi}^{MTU} = 0$ for wrist prime movers (ECR, FCR).

The MTU excursion model at the index finger joints (DIPi, PIPi, MCPi) relied on the normative tendon path data and the geometrical models provided by Chao *et al.* (1989). For finger extensors (EDC), the excursion was determined by considering a constant moment arm. For finger flexors (FDS), the excursion was determined using a bow-string model. The MTU excursion at the wrist joint was determined using regression equation taken from Lemay & Crago (1996).

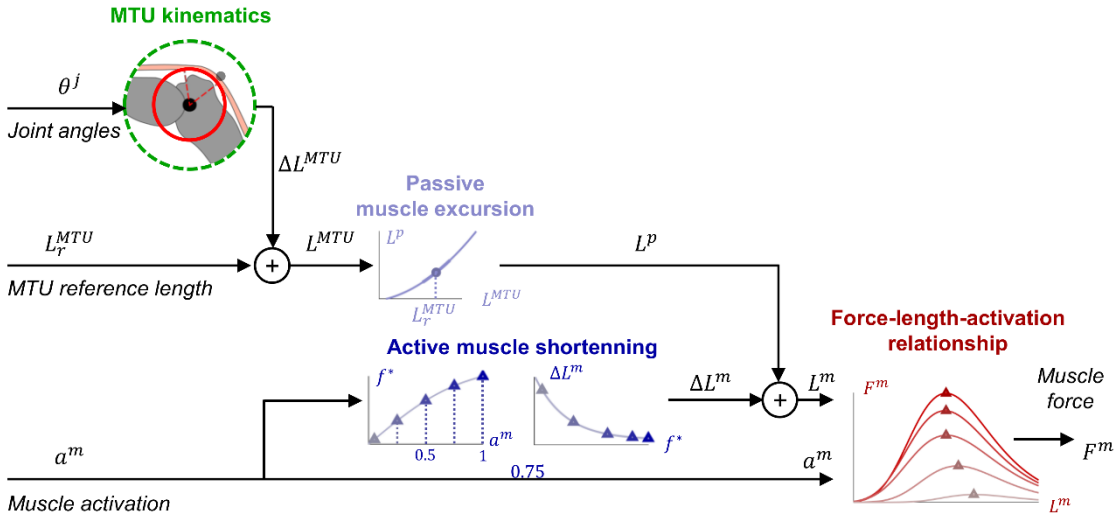

Figure s3-7. Illustration describing the Force-Length-Activation model principle. All symbols and variables are described in the text.

Step 2 - muscle belly excursion

The current muscle belly length (L^m) was determined removing the active muscle belly shortening (ΔL^m) from the passive belly length (L^p), i.e., before contraction.

$$L^m = L^p - \Delta L^m \qquad \text{Equation 2}$$

The passive belly length varies with the tendon lengthening/shortening when joint posture changes and was described here as a function of the current MTU length:

$$L^p(L^{mtu}) = p_2(L^{mtu})^2 + p_1 L^{mtu} + p_0 \quad \text{Equation 3}$$

Where $\boldsymbol{d} = \{d_2; d_1; d_0\}$ are polynomial coefficients that were determined in previous studies(Goislard de Monsabert et al., 2020; Hauraix et al., 2018) from ultrasound imaging and motion capture experimental data. The values of those coefficients are provided in Table s3-1.

The active muscle belly shortening (ΔL^m), corresponding to muscle length decrease with active contraction of the fibres was determined from activation (a^m) with two relationships. The first relationship estimates a virtual muscle force level (f^*) using a sigmoid function (Equation 4).

$$F^*(a^m) = \alpha_1 \left[\frac{1}{1 + exp\left(-\alpha_2 \left(a^m - \alpha_3\right)\right)} - 0.5\right] + \alpha_4 \quad \text{Equation 4}$$

Where $\boldsymbol{\alpha} = \{\alpha_3; \alpha_2; \alpha_1\}$ are coefficients describing the sigmoid function that were determined in previous studies from electromyography and dynamometry experimental data (Goislard de Monsabert et al., 2020; Hauraix et al., 2018). The values of those coefficients are provided in Table s3-2. The second relationship estimates the muscle active shortening ΔL^m during contraction from the virtual force level and was described by an exponential function (Equation 5).

$$\Delta L^m(F^*) = \gamma_1 \left[1 - exp(-\gamma_2 F^*)\right] \quad \text{Equation 5}$$

Where $\boldsymbol{\gamma} = \{\gamma_2; \gamma_1\}$ are coefficients describing the exponential function and were determined in previous studies from dynamometry, ultrasound and motion capture experimental data (Goislard de Monsabert et al., 2020; Hauraix et al., 2018). The values of those coefficients are provided in Table s3-3.

Step 3 - Force-length-activation relationship

The muscle force was estimated from muscle belly length (L^m) and muscle activation (a^m) using a force-length-activation relationship. This relationship relied on the equations of Kaufman et al.(1989) (Equations 7a-d) describing force-length behaviour at maximal activation ($a^m = 1$) and was adapted to include activation-dependency of the three parameters, i.e., index of architecture (i_a), optimal belly length (L_0) and maximal isometric force (F_0) (Equations 6a-c). The first step was thus to compute these parameters using the following polynomial relationship

$$i_a = b_5(a^m)^5 + b_4(a^m)^4 + b_3(a^m)^3 + b_2(a^m)^2 + b_1 a^m + b_0 \quad \text{Equation 6a}$$

$$L_0 = c_5(a^m)^5 + c_4(a^m)^4 + c_3(a^m)^3 + c_2(a^m)^2 + c_1 a^m + b_0 \quad \text{Equation 6b}$$

$$F_0 = d_3(a^m)^3 + d_2(a^m)^2 + d_1 a^m \quad \text{Equation 6c}$$

Where $\boldsymbol{b} = \{b_5; b_4; b_3; b_2; d_1; d_0\}$, $\boldsymbol{c} = \{c_3; c_2; c_1; c_0\}$ and $\boldsymbol{d} = \{d_3; d_2; d_1; d_0\}$ are polynomial coefficients that were determined in previous studies (Goislard de Monsabert et al., 2020; Hauraix et al., 2018). The values of those coefficients are provided in Table s3-4, s3-5 and s3-6. Muscle force was then estimated from muscle belly length using the calculated parameters in the equation of Kaufman *et al*.

$$F^m(L^m) = F_0 . exp\left[-\left(\frac{(\varepsilon^m + 1)^\beta - 1}{\omega}\right)^\rho\right] \quad \text{Equation 7a}$$

with

$$\varepsilon^m = \frac{L^m - L_0}{L_0} \quad \text{Equation 7b}$$

$$\omega = 0.35327(1 - i_a) \quad \text{Equation 7c}$$

$$\beta = 0.96343\left(1 - \frac{1}{i_a}\right) \quad \text{Equation 7d}$$

Where ε^m was the muscle strain and ω, β and ρ were shape parameters of the force-length relationship corresponding to width, skewness, and roundness, respectively. Roundness ρ was equal to 2 (Goislard de Monsabert et al., 2020; Hauraix et al., 2018).

Associated data

Table s3-2 – Coefficients of the polynomial regression between normalized passive belly length (l^p) and normalized muscle-tendon unit length (l^{mtu}). To use as follows $l_1^m = p_2(l^{mtu})^2 + p_1 l^{mtu} + p_0$. Muscle-tendon unit length was normalized by dividing by the reference muscle-tendon unit length (L_r^{MTU}). Passive muscle belly length was normalized by dividing it by its value at reference posture, i.e., using $L^{MTU} = L_r^{MTU}$ in equation 2.

	p2	p1	p0
FCR	-0.66	2.70	-1.05
ECR	25.97	-48.21	23.25
EDC	15.71	-29.60	14.90

Table s3-3 – Coefficients of the relationship between normalized virtual force (f^*)and muscle activation (a^m). To use as follows: $f^*(a^m) = \alpha_1 \left[\frac{1}{1+exp^{-\alpha_2 (a^m - \alpha_3)}} - 0.5\right] + \alpha_4$.Virtual force was normalized by dividing by F^{max}, i.e., the maximal isometric force F^0 at maximal activation ($a^m = 1$). Muscle activation a^m was unitless and equal to 1 during a maximal voluntary contraction.

	α_1	α_2	α_3	α_4
FCR	0	0	2.07	2.95
ECR	0.096	0.13	2.01	2.72
EDC	0.33	0.40	1.27	4.47

Table s3-4 – Coefficients of the relationship between normalized muscle active shortening (Δl^m) and normalized virtual force f^*. To use as follows: $\Delta l^m(f^*) = \gamma_1 [1 - exp(-\gamma_2 f^*)]$. Virtual force was normalized by dividing by F^{max}, i.e., the maximal isometric force F^0 at maximal activation ($a^m = 1$). Muscle active shortening was normalized by dividing by passive muscle belly length at reference posture, i.e., using $L^{MTU} = L_r^{MTU}$ in equation 2. A positive Δl^m corresponds to muscle shortening.

	γ_1	γ_2
FCR	0.043	4.37
ECR	0.069	3.61
EDC	0.028	3.72

Table s3-5 – Coefficients of the polynomial regression between the index of architecture (i_a) and the activation level (a^m). The coefficients are used as follows: $i_a = b_5(a^m)^5 + b_4(a^m)^4 + b_3(a^m)^3 + b_2(a^m)^2 + b_1a^m + b_0$. Muscle activation a^m was unitless and equal to 1 during a maximal voluntary contraction. Index of architecture i_a was unitless.

	b_5	b_4	b_3	b_2	b_1	b_0
FCR	0.714	-2.399	2.463	-0.701	0.069	0.169
ECR	-0.664	2.575	-3.404	1.712	-0.157	0.231
EDC	-0.105	0.308	-0.697	0.792	-0.167	0.173

Table s3-6 – Coefficients of the polynomial regression between normalized optimal length (l_0) and muscle activation (a^m). To use as follows: $l_0 = c_5(a^m)^5 + c_4(a^m)^4 + c_3(a^m)^3 + c_2(a^m)^2 + c_1a^m + c_0$. Optimal length L_0 was normalized by dividing by the passive muscle belly length at reference posture, i.e., using $L^{MTU} = L_r^{MTU}$ in equation 2. Muscle activation a^m was unitless and equal to 1 during a maximal voluntary contraction. Index of architecture i_a was unitless.

	c_5	c_4	c_3	c_2	c_1	c_0
FCR	0.096	-0.335	0.330	-0.042	-0.099	1.002
ECR	0	0	-0.048	0.196	-0.211	0.971
EDC	0	0	-0.050	0.107	-0.083	1.016

Table s3-7 – Coefficients of the polynomial regression between the normalised maximal force (f_0) and the activation level (a^m). The coefficients are used as follows: $f_0 = d_3(a^m)^3 + d_2(a^m)^2 + d_1a^m$. Maximal force was normalized by dividing by F^{max}, i.e., the maximal isometric force F^0 at maximal activation ($a^m = 1$)

	d_3	d_2	d_1
FCR	0.297	-1.430	2.120
ECR	-0.029	-0.336	1.361
EDC	-0.528	0.025	1.484

References

Chao, E. Y., An, K. N., Cooney III, W. P., & Linscheid, R. L. (1989). *Biomechanics of the hand : A basic research study*. World Scientific.

Goislard de Monsabert, B., Hauraix, H., Caumes, M., Herbaut, A., Berton, E., & Vigouroux, L. (2020). Modelling force-length-activation relationships of wrist and finger extensor muscles. *Medical & Biological Engineering & Computing*, *58*(10), 2531-2549. https://doi.org/10.1007/s11517-020-02239-0

Hauraix, H., Goislard De Monsabert, B., Herbaut, A., Berton, E., & Vigouroux, L. (2018). Force–Length Relationship Modeling of Wrist and Finger Flexor Muscles. *Medicine & Science in Sports & Exercise*, *50*(11), 2311-2321. https://doi.org/10.1249/MSS.0000000000001690

Kaufman, K. R., An, K. N., & Chao, E. Y. (1989). Incorporation of muscle architecture into the muscle length-tension relationship. *Journal of Biomechanics*, *22*(8-9), 943-948.

Lemay, M. A., & Crago, P. E. (1996). A dynamic model for simulating movements of the elbow, forearm, and wrist. *Journal of Biomechanics*, *29*(10), 1319-1330. https://doi.org/16/0021-9290(96)00026-7